

Effect of Additional Surfaces on Ordinary Portland Cement Early-Age Hydration

Tapio Vehmas^{1*}, Anna Kronlöf², Andrzej Cwirzen³

¹VTT Technical Research Centre of Finland Ltd., Espoo, Finland

²VTT Expert Services Oy, Espoo, Finland

³Department of Civil, Environmental and Natural Resources Engineering, Luleå University of Technology, Luleå, Sweden

Email: *tapio.vehmas@vtt.fi

How to cite this paper: Vehmas, T., Kronlöf, A. and Cwirzen, A. (2017) Effect of Additional Surfaces on Ordinary Portland Cement Early-Age Hydration. *Materials Sciences and Applications*, 8, 859-872. <https://doi.org/10.4236/msa.2017.812063>

Received: September 18, 2017

Accepted: November 7, 2017

Published: November 10, 2017

Copyright © 2017 by authors and Scientific Research Publishing Inc. This work is licensed under the Creative Commons Attribution International License (CC BY 4.0).

<http://creativecommons.org/licenses/by/4.0/>



Open Access

Abstract

Early-age hydration of Ordinary Portland Cement (OPC) was studied in the presence of two additional surfaces. Additional surfaces are known to accelerate the early-age hydration of OPC. Autocatalytic reaction modelling was used to determine acceleration mechanism of additional surfaces. Heat development of the hydration was measured with semi-adiabatic calorimetry and the results were modelled with an autocatalytic reaction. Autocatalytic reaction modelling was able to determine number of initially active nucleation sites in early-age hydration. OPC hydration followed autocatalytic reaction principles throughout induction period and accelerating period. Both of the added surfaces, limestone filler and calcium-silicate-hydrate (C-S-H) coated limestone filler accelerated the early-age hydration. According to autocatalytic modelling, the C-S-H coated filler increased the number of initially active nucleation sites. Pristine limestone filler accelerated the early-age hydration by providing the additional nucleation sites throughout the early-age hydration. The difference was explained with common theories of nucleation and crystal growth. Autocatalytic model and measured calorimeter curve started to significantly deviate at the inflection point, where the reaction mode changed. The reaction mode change depended on the average particle distance. Early-age hydration, modelled as autocatalytic reaction was able to improve understanding of OPC early-age hydration and quantify the number of initially active nucleation sites. Understanding and quantifying the acceleration mechanisms in early-age hydration will aid larger utilization of supplementary cementitious materials where understanding the early-age strength development is crucial.

Keywords

Ordinary Portland Cement, Hydration, Early-Age, Surfaces,

1. Introduction

In recent decades, nucleation and crystal growth mechanisms has received an ever strengthening position as the explanation of hydration phenomena of Ordinary Portland Cement (OPC) [1]. It is largely recognized that cement hydration can be divided into various stages: initial dissolution, induction period, accelerating period and deceleration period [1] [2]. Earlier, application of classical crystal growth theories [3] [4] failed to explain slow hydration during the induction period without additional hindering process. This hindering process has been explained with formation of membranes with meta-stable layers and their later rupture. During the past decade, the fundamental work of Nonat and others [5]-[12] cast doubt on the existence of membranes. Recently, Thomas adapted a modified Avrami crystal growth model [3] and successfully explained the origin of the induction period as a part of a crystallization process, without a need for additional hindering mechanism. At present, a massive body of experimental and modelling studies supports theory that a slow reaction stage, the induction period, is related to a small number of active growth sites of calcium-silicate-hydrate. Also formation of membranes is observed and modelled [13] [14]. Further evidence for nucleation models were gained from addition of artificial growth sites of calcium-silicate-hydrate by Thomas *et al.*, in the form of a pre-precipitated calcium-silicate-hydrate (C-S-H) [15].

A number of authors indicated that the rate of OPC hydration depended on the amount of reaction products, which is analogous to the autocatalytic reaction [16] [17] [18]. It has been also observed that various fine materials accelerated hydration processes [19] [20] [21] [22] [23]. According to the autocatalytic reaction theory, the reaction product acts as catalysis for further reaction by accelerating the reaction (Equation (1)). This type of reaction exhibits an S-shaped correlation between the amounts of reaction product and the time. In the pseudo-first-order reaction, the reaction rate can be expressed as a sum of a two-stage reaction (Equation (2)):



$$k = k_1 [A] + k_2 [A][B] \quad (2)$$

where $[A]$ represents a concentration of initial materials and $[B]$ represents a concentration of formed reaction products. k_1 and k_2 coefficients take into account the reaction rates. The autocatalytic reaction includes initiation of the reaction (reaction rate coefficient k_1) followed by the autocatalytic reaction (reaction rate coefficient k_2). These two reactions can be described as non-catalytic and autocatalytic, respectively. In the Ordinary Portland Cement hydration, the primary nucleation step occurs following early dissolution of tri-calcium silicate

and precipitation stages of calcium-silicate-hydrates (C-S-H) [6] [7]. Within the first approximately 15 min, the process consists of the dissolution of calcium and silicate up to their maximum supersaturation level along with the primary precipitation of C-S-H nuclides. This can be considered as the non-catalytic stage of reaction which later initiates the second stage reaction, the crystal growth of C-S-H. As the duration of the period of the primary nucleation step is negligible compared to the reaction period examined here, the non-catalytic-reaction in Equation (1) can be replaced with the quantity of C-S-H formed initially during the primary nucleation step $[B_0]$. The quantity of formed reaction product $[B]$ at given time can be expressed as a simple mathematical equation for autocatalytic reaction (Equation (3)):

$$[B] = \frac{[B_0] + [A_0]}{1 + \frac{[A_0]}{[B_0]}} e^{-([A_0] - [B_0])k_2 t} - [B_0] \quad (3)$$

where $[A_0]$ represents an overall initial material concentration, t is the time from initial nucleation and k_2 is the reaction rate coefficient of autocatalytic reaction. The main objective of the present study was to analyze the effects of various surfaces on early-age hydration of Portland cement using calorimetric data combined with the autocatalytic reaction model of the C-S-H phase.

2. Materials and Methods

The used cement was white Ordinary Portland Cement type CEM I 52,5 R, from Aalborg. The limestones fillers, type SB63, were produced by Nordkalk Oy. The provided fillers had different finesses and are commonly used in self-compacting concrete in Finland. Chemical compositions of used cement and limestone filler are shown in **Table 1**. Particle distributions were measured with a Beckman Coulter LS particle size analyzer. The specific surface areas (SSA) were calculated from the particle size distributions (**Figure 1**).

Calcium-silicate-hydrate (C-S-H) coated limestone was produced by vigorously mixing $\text{Na}_2(\text{SiO}_2)_{3,3}$ and $\text{Ca}(\text{OH})_2$ respectively to water in the presence of limestone filler. The used $\text{Ca}(\text{OH})_2$ was purchased from Fluka analytical and $\text{Na}_2(\text{SiO}_2)_{3,3}$ from Huber engineered materials (Zeopol 33). The amounts of reactants in the solution were defined to produce a layer with the average thickness of 8.4 nm. The density of the layer was expected to be 2.6 mg/m^3 according to the formula $(\text{CaO})_{1,7}(\text{SiO}_2)(\text{H}_2\text{O})_{1,8}$ [24].

After precipitation of the C-S-H limestone fillers were immediately washed three times with 5 mM $\text{Ca}(\text{OH})_2$ which was saturated in respect to silicon. Washing was done in order to remove sodium. Both, coating and washing processes were monitored with conductometer (Radiometer analytical, CDM 2010) to ensure similar processing. Solution was separated by decantation and the excess water was evaporated from the slurry by drying at 40°C until the water content was sufficiently low to produce pastes. The successfulness of coverage of limestone with C-S-H was verified by JEOL Scanning Electron Microscope

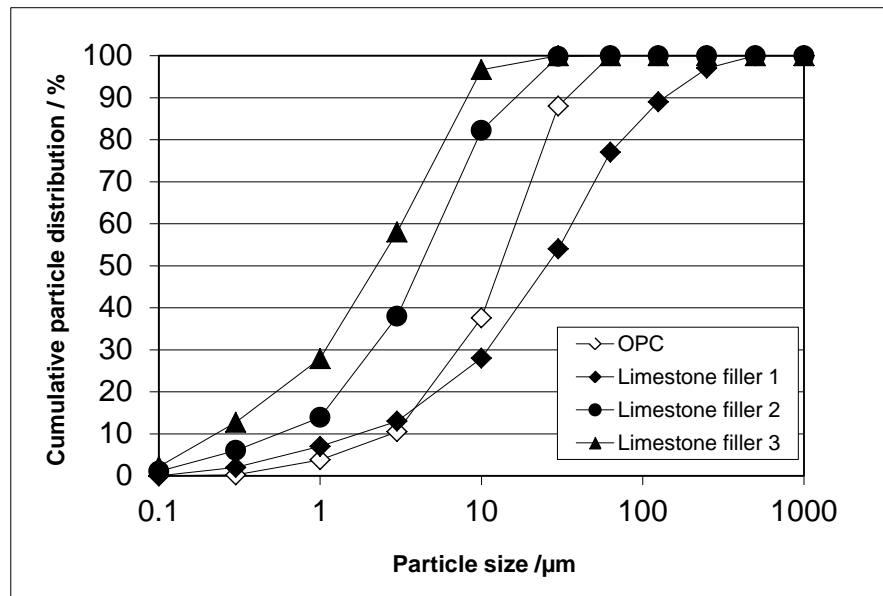


Figure 1. Grading curves for used materials. The specific surface areas calculated from the size distributions were OPC: 609 m²/kg; limestone filler 1: 376 m²/kg; limestone filler 2: 1648 m²/kg; and limestone filler 3: 2930 m²/kg.

Table 1. Compositions of used white ordinary Portland cement and limestone.

Elemental composition	CEM I 52.5R	Limestone
CaO	69%	48%
SiO ₂	25%	6%
Al ₂ O ₃	2.1%	1.0%
Fe ₂ O ₃	0.3%	0.6%
MgO	0.7%	3.6%
SO ₃	0.3%	-
Ignition loss	<1%	40%

(Figure 2). Pastes were prepared by mixing all dry materials for 1 min, followed by addition of the tempered water in the next 30 s. The total mixing time was 5 minutes. Samples were placed into a semi-adiabatic calorimeter 15 min after mixing. It was assumed that the initial heat of dissolution was lost and the observed heat originated from silicate based reactions [25]. Heat capacities were calculated and the experiments conducted according standard procedure [26] with two parallel samples. The experimental mixes are listed in Table 2.

The heat output rate at the increasing temperature of the semi-adiabatic conditions was normalized to constant temperature with Arrhenius equation using the value of 33 kJ/mol for the apparent activation energy [26] [27].

The autocatalytic reaction Equation (3) was fitted to the normalized calorimeter curves using the Excel solver function. Assuming that observed hydration heat was proportional to the formation of C-S-H, $[B]$ represented the formed calcium-silicate-hydrate and $[B_0]$ the quantity of the initially formed C-S-H. $[A_0]$

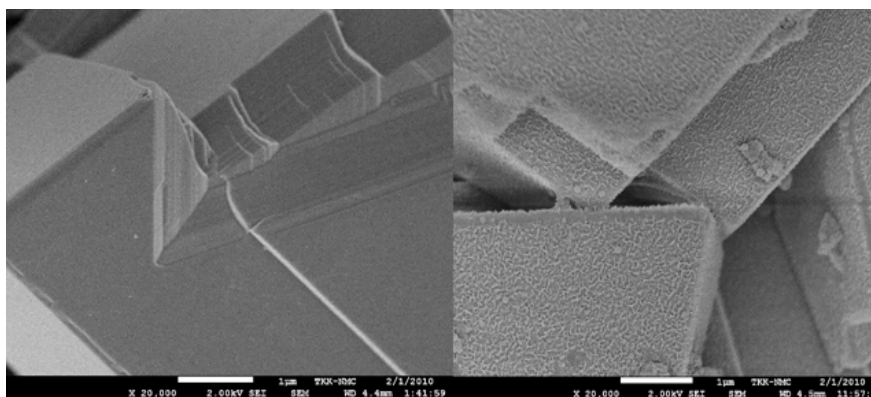


Figure 2. Scanning electron microscope images of uncoated calcite surface (left) and C-S-H coated calcite surface (right). The coating in the image was made on pure precipitated calcite in order to better illustrate the surface details produced by the C-S-H coating.

Table 2. Compositions of studied pastes.

Materials	Water/cement-ratio	Water/powder-ratio	Surface area (m ² /m ³)
OPC	0.30	0.30	870
OPC	0.40	0.40	750
OPC	0.50	0.50	660
OPC	0.60	0.60	580
OPC/Limestone 3	0.50	0.43	680
OPC/Limestone 3	0.50	0.38	700
OPC/Limestone 3	0.50	0.31	760
OPC/Limestone 3	0.50	0.23	810
OPC/Limestone 2	0.50	0.39	1190
OPC/Limestone 2	0.50	0.32	1600
OPC/Limestone 2	0.50	0.24	2170
OPC/Limestone 1	0.50	0.38	1790
OPC/Limestone 1	0.50	0.31	2620
OPC/Limestone 2 CSH	0.50	0.39	1190*
OPC/Limestone 2 CSH	0.50	0.32	1600*
OPC/Limestone 3 CSH	0.50	0.24	2170*

*Surface area of limestone filler prior CSH coating.

was chosen the arbitrarily as a value of 400 kJ/kg based on manufacturers information. Fitting was done by enabling a free variation of constant representing a number of initial C-S-H nuclei [B_0] and reaction rate constant k_2 . The curves exhibited a clear knee point limiting the extent of fitting. According to Equation (3), [B_0] is responsible for the early start-up of the reaction and k_2 for its later propagation. If the reaction would follow the autocatalytic mode precisely, the value of the reaction rate coefficient (k_2) would yield a constant value. Any deviation of (k_2) indicates that the reaction propagates slower or faster than expected

according to the model alone. Example of calorimeter curves and autocatalytic modelling are in **Figure 3**.

The end of the accelerating period was determined by maximum value of the heat rate, which denotes the end of accelerating period and beginning of decelerating period. This point was named as the inflection point.

3. Results

Addition of limestone fillers accelerated heat evolution in all studied samples. Even greater acceleration was observed when C-S-H coated limestone was used. The application of the autocatalytic model to the heat output revealed that the quantity of the initial C-S-H, $[B_0]$ increased as the water/cement-ratio (w/c) increased (**Figure 4**). Addition of limestone filler increased the total surface area to the mix but did not affect the quantity of the formed C-S-H. On the contrary

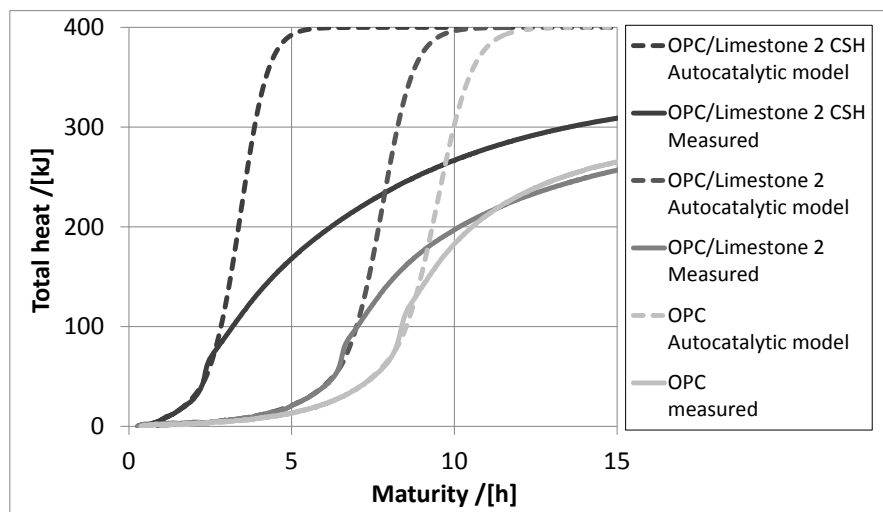


Figure 3. Measured semi-adiabatic calorimetric curves and modelled autocatalytic curves.

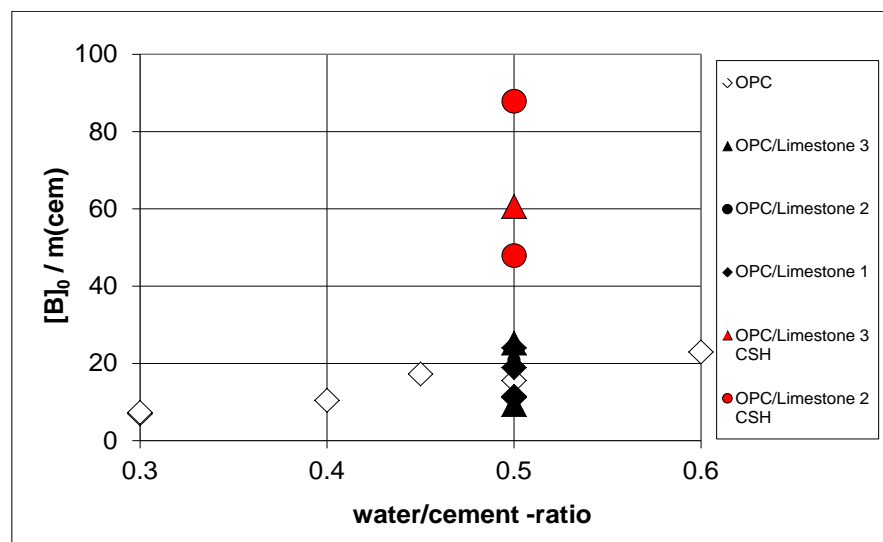


Figure 4. Modelled number of active C-S-H growth sites and water/cement-ratio.

addition of the C-S-H coated limestone filler increased the quantity of the C-S-H significantly (**Figure 5**). This quantity increased up to 4.5 fold compared to the uncoated limestone or pure cement pastes. The autocatalytic reaction rate coefficient k_2 decreased as w/c-ratio increased but increased in the presence of limestone fillers and C-S-H coated limestone fillers (**Figure 6**) (**Figure 7**).

The heat output at the inflection point (point where the reaction rate began to decrease) increased as the w/c-ratio increased. Addition of limestone and C-S-H coated limestone appeared to decrease the heat output (**Figure 8**).

4. Discussion

Although the experiments were made with white Ordinary Portland Cement and grounded limestone, the cement hydration followed the autocatalytic reaction

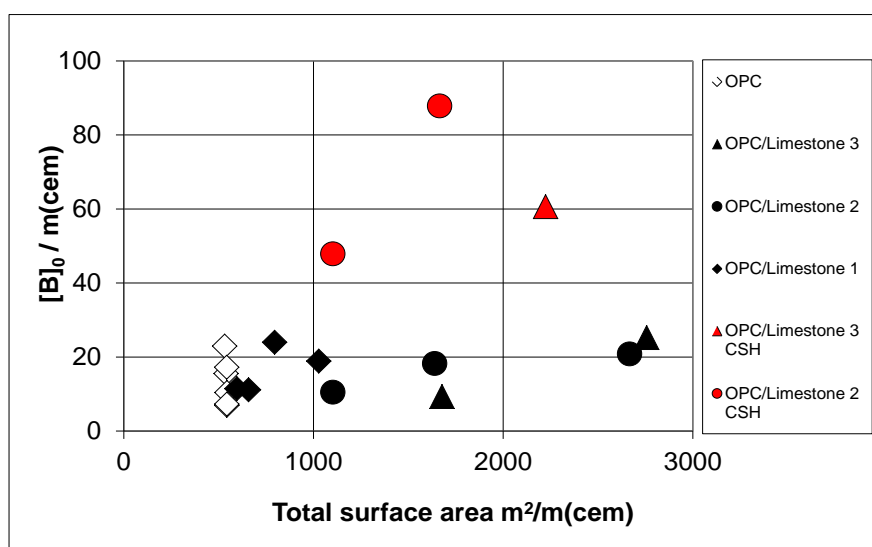


Figure 5. Modelled number of active C-S-H growth sites and total surface area.

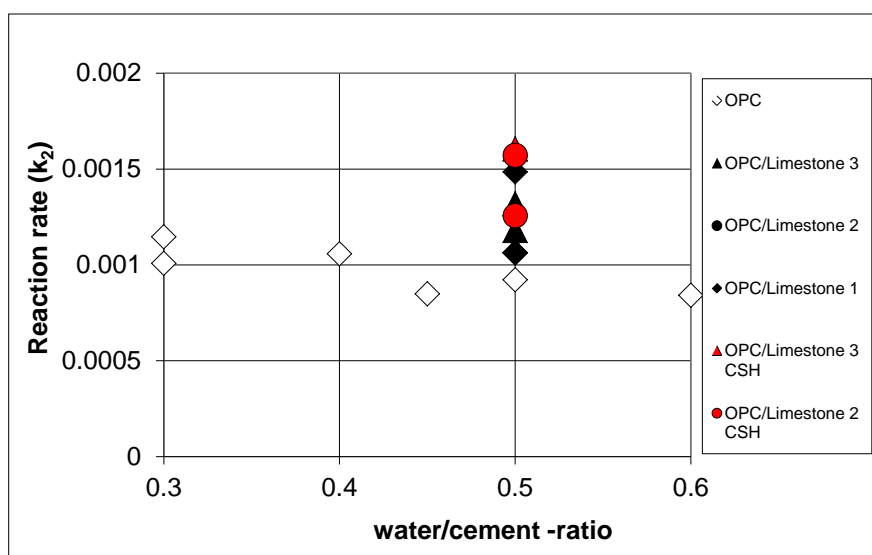


Figure 6. Modelled autocatalytic reaction rate (k_2) and water/cement-ratio.

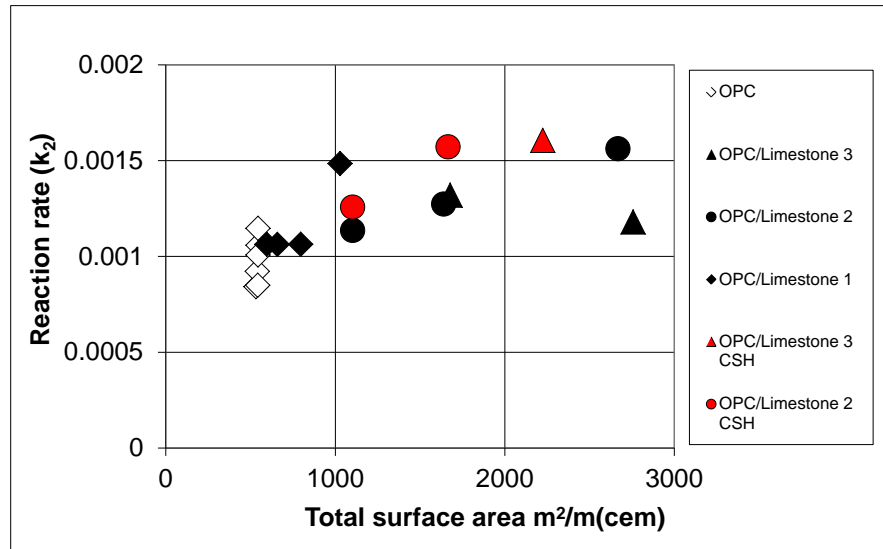


Figure 7. Modelled autocatalytic reaction rate (k_2) and total surface area.

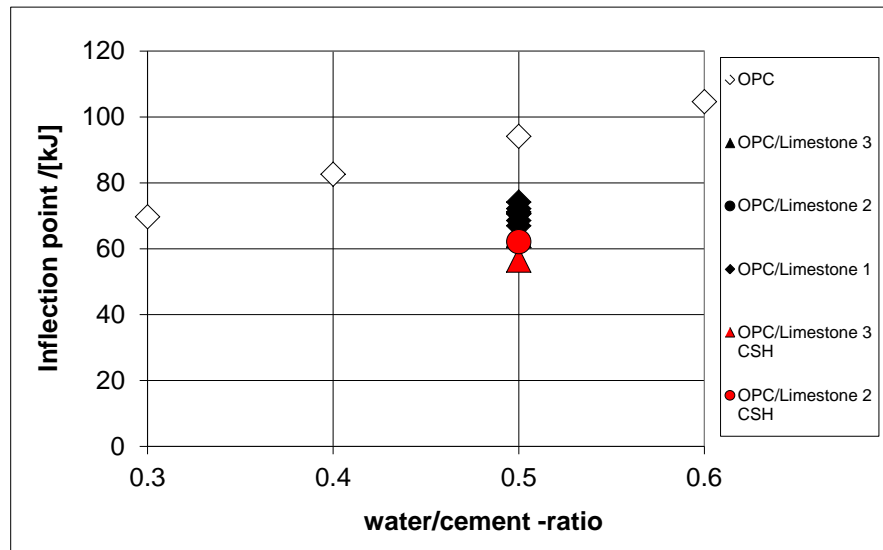


Figure 8. Inflection point and water/cement-ratio.

principles within the first hours. An excellent fitting for autocatalytic model was observed throughout the induction period and the acceleration period. Excellent fitting does not confirm the autocatalytic nature of the early-age hydration. Multiple models match the sigmoidal shape of the curve, producing the so-called sigmoidal fraud [28]. However, according to the obtained results the autocatalytic nature of the early-age hydration is plausible. The autocatalytic reaction and measured calorimeter curves started to significantly deviate near the point where accelerating period changed to deceleration period. This point was named as an inflection point. After the inflection point, the measured calorimeter data and autocatalytic model showed clear differences. The studied samples produced significantly less heat compared to the autocatalytic model in the deceleration period. This probably indicates some change of the reaction mechanism.

According to the autocatalytic modelling, the quantity of the initial C-S-H increased as the w/c-ratio increased in pure cement pastes. This observation complied with earlier studies, stating that the quantity of the initial C-S-H depends on the amount of the supersaturated silicon in the first dissolution step [6].

As limestone fillers were introduced to the mixes, the quantity of the C-S-H formed initially did not increase according to the autocatalytic modelling. However, in the presence of the C-S-H coated limestone filler, the increase was up to 4.5 times higher in comparison with the uncoated filler and pure paste. The result indicated that the C-S-H coating acted as nucleation sites from the very beginning of the measuring period.

Towards the end of the acceleratory period in the presence of the filler surfaces, the reaction propagated faster than could be expected according to the autocatalytic reaction alone. The increased nonlinear propagation of the reaction was impossible to explain by increasing the quantity of C-S-H formed initially. Consequently, a deviation from the autocatalytic model in the reaction rate coefficient (k_2) was introduced. The higher reaction rate could be a consequence of an additional C-S-H nucleation which followed the primary nucleation. The additional C-S-H nucleation could take place simultaneously with the autocatalytic reaction. The difference is that C-S-H growth on C-S-H does not need additional energy but the C-S-H growth on mineral surfaces must overcome energy barrier. This energy barrier is known in nucleation and crystal growth theories when materials precipitate on foreign substrate. Crystallization from solutions underlies in a large range of industrial, laboratory and physiological processes [29]. The precipitation process over a certain energy barrier is expressed by Equation (4) [18]:

$$I^h = K^h \exp\left(\frac{-\Delta G_k^h}{RT}\right) \quad (4)$$

I^h is the rate of nucleation in a unit area of substrate. K^h is a constant irrespective of the substrate type, presenting nucleation rate without energy barrier. R is the universal gas constant. T is a temperature and ΔG_k^h is a potential energy barrier for heterogeneous nucleation which can also be expressed as shown in Equation (5), [5] [18] [30]:

$$\Delta G_k^h = \Delta G_k \frac{(2 + \cos \Theta)(1 - \cos \Theta)^2}{4} \quad (5)$$

where ΔG_k is the potential energy barrier for a homogeneous nucleation and θ is the contact angle between the nucleating crystal and the substrate. When the substrate is identical to nucleating crystal, $\theta = 0^\circ$ and no potential barrier exist. If the substrate does not have any similarities to nucleating crystals, then $\theta = 180^\circ$ and additional nucleation rate is similar to a homogeneous nucleation. According to the classic nucleation theory, the potential barrier for a homogeneous nucleation can be related to the degree of supersaturation as expressed in Equation (6), [31]:

$$\Delta G_k = 4\pi r^2 \sigma - \frac{4\pi r^3}{3v_a} RT \ln \left(\frac{Q}{K_{sp}} \right) \quad (6)$$

r is the radius of nucleating product, σ is the surface tension related to the product, v is the molar volume of the product, Q is the ion activity product in the supersaturated solution and K_{sp} is the solubility product of a calcium-silicate-hydrate.

The values of surface tension (σ) of a nucleating C-S-H, molar volume (v) and radius (r) were determined by Gauffinet and Nonat [5]. The contact angle (θ) between calcite and C-S-H was calculated to be 60° [5], which further yields the relative nucleation rate ($f^{\#}$) a value 0.13 at the equilibrium saturation. According to calculations, additional nuclides on filler surfaces are able to precipitate during the crystal growth of calcium silicate hydrates. The larger surface area of fillers in the mixes, the larger is the deviation of reaction rate k_2 (Figure 7). According to calculations, this deviation originates further nucleation of C-S-H on mineral filler surfaces.

Since the filler surfaces perform as active nucleation sites for the C-S-H formation the hydration products will be also deposited on these surfaces along with the OPC surfaces. Consequently, a formation of a thinner product layer on OPC could be expected in the presence of fillers. The total product volume should remain the same. The calorimetric test results revealed a decreasing heat evolution at the inflection point in the presence of fillers which contradicts the earlier assumption. The formed layer of hydration product on the OPC surface at the knee point (the time of the change of the reaction mode) appeared to consist of a smaller quantity of product per unit of OPC surface in the presence of fillers when compared to the pure paste. This observation contradicts the wide spread thinking that the knee point corresponds to the formation of a diffusion barrier. The present test results indicate that the origin of the knee point is different. One explanation could be related to the geometry of the particle system particularly the inter particle distances. Generally, the shorter is the distance the smaller is the heat output at the inflection point (Figure 9) and the more limited is the space for C-S-H formation around OPC particles presuming that the particles are distributed evenly. The lack of a free volume around cement particles is related to the onset of the densification of C-S-H beyond a critical point that reduces its efficiency as an autocatalyst. Similar behavior was also observed when the w/c-ratio of pure pastes was varied (Figure 8). Densification of early C-S-H versus time has been observed with SANS measurements by Jennings *et al.* [32]. It has also been modelled by Bishnoi and Scrivener [33].

5. Conclusions

Early-age hydration was studied with semi-adiabatic calorimeter. Effects of temperature rise and heat capacities were normalized in a standard manner. For normalized calorimeter curves, autocatalytic model was fitted with two variable parameters, reaction rate and quantity of initial nuclei. It was observed that

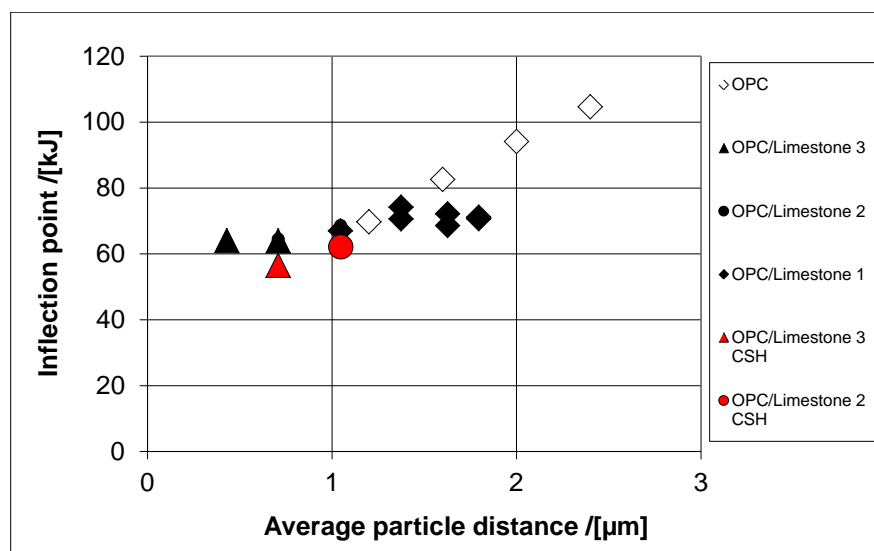


Figure 9. Inflection point and average particle distance.

cement hydration followed autocatalytic reaction principles throughout induction period and accelerating period. Autocatalytic model and measured calorimeter curve started to significantly deviate at the inflection point, where the reaction mode changed. According autocatalytic modelling this type of reaction mode change can be understood as a densification process. In most of the samples, beginning of densification process was observed to depend on the average particle distance.

A simple method to apply autocatalytic reaction was established. It was assumed that autocatalytic material, C-S-H, was formed through supersaturation/precipitation-process during the initial dissolution. It was found to be an accurate approach in terms of modelling of pure cement pastes. As limestone fillers were introduced to the mixes, the quantity of initially formed C-S-H did not increase. In case of C-S-H coated fillers, a huge increase of initially formed C-S-H was observed. The reaction rate of the autocatalytic reaction was increased as additional surface was introduced to samples. The increased reaction rate was related to additional nucleation of C-S-H on the filler surface and simple thermodynamic equations were proposed to evaluate these effects. This type of approach could give a valuable data for cement hydration simulations and microstructural modelling [34] [35], especially in the case of evaluation of effect of supplementary cementitious materials on the early-age hydration.

Acknowledgements

This work was supported by the Finnish Funding Agency for Technology and Innovation, Nordkalk Oy Ab, Cements Ab and Tikkurila Oyj. Authors also wish to thank Dr. Ilya Anoskin of SEM imaging.

References

- [1] Bullard, J.W., Jennings, H.M., Livingston, R.A., Nonat, A., Scherer, G.W., Schweitz-

- er, J.S., *et al.* (2011) Mechanisms of Cement Hydration. *Cement and Concrete Research*, **41**, 1208-1223. <https://doi.org/10.1016/j.cemconres.2010.09.011>
- [2] Scrivener, K.L. and Nonat, A. (2011) Hydration of Cementitious Materials, Present and Future. *Cement and Concrete Research*, **41**, 651-665. <https://doi.org/10.1016/j.cemconres.2011.03.026>
- [3] Thomas, J.J. (2007) A New Approach to Modeling the Nucleation and Growth Kinetics of Tricalcium Silicate Hydration. *Journal of the American Ceramic Society*, **90**, 3282-3288. <https://doi.org/10.1111/j.1551-2916.2007.01858.x>
- [4] Brown, P.W., Pommersheim, J. and Frohnsdorff, G. (1985) A Kinetic Model for the Hydration of Tricalcium Silicate. *Cement and Concrete Research*, **15**, 35-41. [https://doi.org/10.1016/0008-8846\(85\)90006-7](https://doi.org/10.1016/0008-8846(85)90006-7)
- [5] Garrault-Gauffinet, S. and Nonat, A. (1999) Experimental Investigation of Calcium Silicate Hydrate (C-S-H) Nucleation. *Journal of Crystal Growth*, **200**, 565-574. [https://doi.org/10.1016/S0022-0248\(99\)00051-2](https://doi.org/10.1016/S0022-0248(99)00051-2)
- [6] Garrault, S. and Nonat, A. (2001) Hydrated Layer Formation on Tricalcium and Dicalcium Silicate Surfaces: Experimental Study and Numerical Simulations. *Langmuir*, **17**, 8131-8138. <https://doi.org/10.1021/la011201z>
- [7] Garrault, S., Behr, T. and Nonat, A. (2006) Formation of the C-S-H Layer during Early Hydration of Tricalcium Silicate Grains with Different Sizes. *The Journal of Physical Chemistry B*, **110**, 270-275. <https://doi.org/10.1021/jp0547212>
- [8] Labbez, C., Nonat, A., Pochard, I. and Jönsson, B. (2007) Experimental and Theoretical Evidence of Overcharging of Calcium Silicate Hydrate. *Journal of Colloid and Interface Science*, **309**, 303-307. <https://doi.org/10.1016/j.jcis.2007.02.048>
- [9] Nonat, A. (2004) The Structure and Stoichiometry of C-S-H. *Cement and Concrete Research*, **34**, 1521-1528. <https://doi.org/10.1016/j.cemconres.2004.04.035>
- [10] Nonat, A., Mutin, J.C., Lecoq, X. and Jiang, S.P. (1997) Physico-Chemical Parameters Determining Hydration and Particle Interactions during the Setting of Silicate Cements. *Solid State Ionics*, **101**, 923-930. <https://doi.org/10.1016/j.cemconres.2004.04.035>
- [11] Nonat, A. (1994) Interactions between Chemical Evolution (Hydration) and Physical Evolution (Setting) in the Case of Tricalcium Silicate. *Materials and Structures*, **27**, 187-195. <https://doi.org/10.1016/j.cemconres.2004.04.035>
- [12] Labbez, C., Jönsson, B., Pochard, I., Nonat, A. and Cabane, B. (2006) Surface Charge Density and Electrokinetic Potential of Highly Charged Minerals: Experiments and Monte Carlo Simulations on Calcium Silicate Hydrate. *Journal of Physical Chemistry B*, **110**, 9219-3920. <https://doi.org/10.1021/jp057096+>
- [13] Gallucci, E., Mathur, P. and Scrivener, K. (2010) Microstructural Development of Early Age Hydration Shells around Cement Grains. *Cement and Concrete Research*, **40**, 4-13. <https://doi.org/10.1016/j.cemconres.2009.09.015>
- [14] Bellmann, F., Damidot, D., Möser, B. and Skibsted, J. (2010) Improved Evidence for the Existence of an Intermediate Phase during Hydration of Tricalcium Silicate. *Cement and Concrete Research*, **40**, 875-884. <https://doi.org/10.1016/j.cemconres.2010.02.007>
- [15] Thomas, J.J., Jennings, H.M. and Chen, J.J. (2009) Influence of Nucleation Seeding on the Hydration Mechanisms of Tricalcium Silicate and Cement. *The Journal of Physical Chemistry C*, **113**, 4327-4334. <https://doi.org/10.1021/jp809811w>
- [16] Mata-Perez, F. and Perez-Benito, J.F. (1987) The Kinetic Rate Law for Autocatalytic Reactions. *Journal of Chemical Education*, **64**, 925.

- <https://doi.org/10.1021/ed064p925>
- [17] Skalny, J.P. (1989) *Materials Science of Concrete 1*. American Ceramic Society Inc., Columbus.
- [18] Liu, C. and Shen, W. (1997) Effect of Crystal Seeding on the Hydration of Calcium Phosphate Cement. *Journal of Materials Science: Materials in Medicine*, **8**, 803-807. <https://doi.org/10.1023/A:1018529116330>
- [19] Oey, T., Kumar, A., Bullard, J.W., Neithalath, N. and Sant, G. (2013) The Filler Effect: The Influence of Filler Content and Surface Area on Cementitious Reaction Rates. *Journal of the American Ceramic Society*, **96**, 1978-1990. <https://doi.org/10.1111/jace.12264>
- [20] Hawkins, P., Tennis, P.D. and Detwiler, R.J. *The Use of Limestone in Portland Cement: A State-of-the-Art Review*, EB227. Portland Cement Association, Skokie, Illinois, 2003, 44 p.
- [21] Sato, T. and Diallo, F. (2010) Seeding Effect of Nano-CaCO₃ on the Hydration of Tricalcium Silicate. *Transportation Research Record*, **2141**, 61-67. <https://doi.org/10.3141/2141-11>
- [22] Björnström, J., Martinelli, A., Matic, A., Börjesson, L. and Panas, I. (2004) Accelerating Effects of Colloidal Nano-Silica for Beneficial Calcium-Silicate-Hydrate Formation in Cement. *Chemical Physics Letters*, **392**, 242-248. <https://doi.org/10.1016/j.cplett.2004.05.071>
- [23] Bentz, D.P., Ardani, A., Barrett, T., Jones, S.Z., Lootens, D., Peltz, M.A., *et al.* (2015) Multi-Scale Investigation of the Performance of Limestone in Concrete. *Construction and Building Materials*, **75**, 1-10. <https://doi.org/10.1016/j.conbuildmat.2014.10.042>
- [24] Chen, J.J., Thomas, J.J., Taylor, H.F.W. and Jennings, H.M. (2004) Solubility and Structure of Calcium Silicate Hydrate. *Cement and Concrete Research*, **34**, 1499-1519. <https://doi.org/10.1016/j.cemconres.2004.04.034>
- [25] Hesse, C., Goetz-Neunhoeffler, F. and Neubauer, J. (2011) A New Approach in Quantitative *In-Situ* XRD of Cement Pastes: Correlation of Heat Flow Curves with Early Hydration Reactions. *Cement and Concrete Research*, **41**, 123-128. <https://doi.org/10.1016/j.cemconres.2010.09.014>
- [26] RILEM Technical Committee 119-TCE (1998) Adiabatic and Semi-Adiabatic Calorimetry to Determine the Temperature Increase in Concrete Due to Hydration Heat of Cement. *Materials and Structures*, **30**, 451-464.
- [27] Kada-Benameur, H., Wirquin, E. and Duthoit, B. (2000) Determination of Apparent Activation Energy of Concrete by Isothermal Calorimetry. *Cement and Concrete Research*, **30**, 301-305. [https://doi.org/10.1016/S0008-8846\(99\)00250-1](https://doi.org/10.1016/S0008-8846(99)00250-1)
- [28] Scherer, G.W. (2012) Models of Confined Growth. *Cement and Concrete Research*, **42**, 1252-1260. <https://doi.org/10.1016/j.cemconres.2012.05.018>
- [29] Vekilov, P.G. (2010) Nucleation. *Crystal Growth & Design*, **10**, 5007-5019. <https://doi.org/10.1021/cg1011633>
- [30] Markov, I. (2003) *Crystal Growth for Beginners, Fundamentals of Nucleation Crystal Growth and Epitaxy*. World Scientific Publishing Co. Ltd., Singapore. <https://doi.org/10.1142/5172>
- [31] Vold, R. and Vold, M. (1983) *Colloid and Interface Chemistry*. Addison-Wesley, Reading.
- [32] Thomas, J.J., Allen, A.J. and Jennings, H.M. (2009) Hydration Kinetics and Microstructure Development of Normal and CaCl₂-Accelerated Tricalcium Silicate Pastes.

The Journal of Physical Chemistry C, **113**, 19836-19844.

<https://doi.org/10.1021/jp907078u>

- [33] Bishnoi, S. and Scrivener, K.L. (2009) Studying Nucleation and Growth Kinetics of Alite Hydration Using UIC. *Cement and Concrete Research*, **39**, 849-860.
<https://doi.org/10.1016/j.cemconres.2009.07.004>
- [34] Bentz, D.P. (2006) Modeling the Influence of Limestone Filler on Cement Hydration Using CEMHYD3D. *Cement and Concrete Composites*, **28**, 124-129.
<https://doi.org/10.1016/j.cemconcomp.2005.10.006>
- [35] Thomas, J.J., Biernacki, J.J., Bullard, J.W., Bishnoi, S., Dolado, J.S., Scherer, G.W., *et al.* (2011) Modeling and Simulation of Cement Hydration Kinetics and Microstructure Development. *Cement and Concrete Research*, **41**, 1257-1278.
<https://doi.org/10.1016/j.cemconres.2010.10.004>